

**Large non-Gaussianities with intermediate shapes from quasi-single-field inflation**Xingang Chen<sup>1,2</sup> and Yi Wang<sup>3,4</sup><sup>1</sup>*Center for Theoretical Physics, Massachusetts Institute of Technology, Cambridge, Massachusetts 02139, USA*<sup>2</sup>*Center for Theoretical Cosmology, DAMTP, University of Cambridge, Cambridge CB3 0WA, United Kingdom*<sup>3</sup>*Physics Department, McGill University, Montreal, H3A2T8, Canada*<sup>4</sup>*KITPC, Institute of Theoretical Physics, Chinese Academy of Sciences, Beijing 100190, China*

(Received 16 October 2009; published 11 March 2010)

We study the slow-roll inflation models, where the inflaton slow-rolls along a trajectory whose orthogonal directions are lifted by potentials with masses of order the Hubble parameter. In these models large non-Gaussianities can be generated through the transformation from the isocurvature modes to the curvature mode, once the inflaton trajectory turns. We find large bispectra with a one-parameter family of novel shapes, interpolating between the equilateral and local shape. According to the in-in formalism, the shapes of these non-Gaussianities are different from a simple projection from the isocurvature non-Gaussian correlation functions.

DOI: [10.1103/PhysRevD.81.063511](https://doi.org/10.1103/PhysRevD.81.063511)

PACS numbers: 98.80.Cq, 98.70.Vc

**I. INTRODUCTION**

Inflation [1] is the leading candidate for creating the homogeneous and isotropic universe and generating the primordial density fluctuations for large scale structure. The condition for inflation to happen is that the inflatons stay near the top of the potential for a sufficiently long time, so that the vacuum energy drives the accelerated expansion of the Universe.

Generically, it is found that such a condition needs to be finely-tuned, at least for various types of models that have sensible UV completion [2]. For slow-roll inflation, this means that the generic inflaton potential has a steep shape, characterized by a mass of order the Hubble parameter  $H$ . On the other hand, it is general that the inflaton can roll in a space with multiple light fields. So at least one of the directions needs to be fine-tuned. A combination of these two aspects suggests a generic situation—the inflaton slow rolls along a trajectory whose orthogonal directions are lifted by potentials with masses of order  $H$ . We call this class of models the quasi-single-field inflation. If the inflaton trajectory is straight, this is equivalent to the single field inflation, which generates unobservably small primordial non-Gaussianities [3]. However, as we will show in this paper, once the trajectory turns, large non-Gaussianities with novel shapes can be generated, which are potentially detectable in current and future experiments.

We call the mode in the tangential direction the curvature mode, and the modes in the perpendicular directions the isocurvature modes. The non-Gaussianities that originated from the curvature mode are very small because the potential is flat. Since the isocurvature modes in our model are massive,  $m \sim H$ , and can have large higher order interactions, the non-Gaussian correlation functions of the isocurvature modes can be very large. However, in de Sitter space, the amplitude of the quantum fluctuations of a massive field decays exponentially after horizon exit,

and is also fast oscillating if  $m \gg H$ . This is why such modes are usually not considered. But for  $m \sim H$ , the suppression due to oscillation is only marginal. In the mean while, although the isocurvature amplitude still decays, the part of it that is transferred to the tangential direction through a turning trajectory becomes part of the curvature mode, which remains constant after horizon exit. The non-Gaussianities in the isocurvature modes are thus transferred in this way. This is the main physical picture behind our calculation.

We use the in-in formalism [4] to compute the precise momentum dependence (shapes) of the bispectra. In this formalism, the natural way to implement the transformation from the isocurvature to curvature mode is to introduce a two-point transfer vertex between the two modes. It is then straightforward to do a perturbative calculation for correlation functions according to the usual Feynman diagrams. As we will see, the effect of the transfer vertex is not a simple projection of the three-point function of the isocurvature modes.

During the computation, we find that two equivalent representations of the in-in formalism, namely, the original factorized form and the commutator form, are computationally advantageous in complementary ways. In certain parameter space, each representation encounters spurious divergence either in IR or UV. These divergences are called spurious because they will eventually be cancelled, but significantly complicate the analytical and numerical calculations. They are completely absent, however, when viewed in a different representation.

We find a one-parameter family of bispectrum shapes, lying in between the well-known equilateral and local shape. The shape sensitively depends on the mass of the isocurvature mode; the size depends on the turning angular velocity and the cubic interaction strength among isocurvature modes.

The mechanism that the isocurvature modes, in particular, their non-Gaussianities, can be transferred to the cur-

vature mode through turning trajectory has been pointed out and studied intensively in the past [5–9]. The focus was on the light isocurvature modes with mass much less than  $H$ . These modes do not decay after horizon exit and non-Gaussianities come from nonlinear classical evolution of superhorizon modes in multifield space. The resulting shapes of non-Gaussianities are local. Also note that for multifield slow-roll inflation models, it is found to be very difficult to generate large non-Gaussianities through this mechanism because of the restrictive slow-roll conditions in all directions. Here in the quasi-single-field inflation models, we focus on massive isocurvature fields, which, as we emphasized and will show in details later, are crucial for generating large non-Gaussianities with new intermediate shapes.

## II. THE MODEL, MODE FUNCTIONS, AND TRANSFER VERTEX

We consider a two-field model as an example. It is convenient to write the action in terms of the fields in polar coordinates,  $\theta$  and  $\sigma$ , that are tangential and orthogonal to the turning trajectory, respectively,

$$S = \int d^4x \sqrt{-g} \left[ \frac{1}{2} (R + \sigma)^2 g^{\mu\nu} \partial_\mu \theta \partial_\nu \theta + \frac{1}{2} g^{\mu\nu} \partial_\mu \sigma \partial_\nu \sigma - V_{\text{sr}}(\theta) - V(\sigma) \right], \quad (1)$$

where  $R$  is the radius of the turning trajectory. The  $V_{\text{sr}}(\theta)$  is a usual slow-roll potential and we choose the rolling velocity  $\dot{\theta}_0 > 0$ . The potential

$$V(\sigma) = \frac{1}{2} m_\sigma^2 \sigma^2 + \frac{1}{6} V''' \sigma^3 + \dots \quad (2)$$

traps the  $\sigma$  field at  $\sigma = 0$  [10]. In principle, the parameters that characterize the turning trajectory,  $\dot{\theta}_0$  and  $R$ , and the cubic interaction strength  $V'''$ , can vary along the trajectory. In this paper, we consider the constant turn case in which they are all constant.

We perform the perturbation in the gauge where the scale factor  $a(t)$  is homogeneous. The leading kinematic Hamiltonian density for the quantum fluctuations,  $\delta\theta_I$  and  $\delta\sigma_I$ , in the interaction picture is

$$\mathcal{H}_0 = a^3 \left[ \frac{1}{2} R^2 \delta\theta_I^2 + \frac{R^2}{2a^2} (\partial_i \delta\theta_I)^2 + \frac{1}{2} \delta\sigma_I^2 + \frac{1}{2a^2} \times (\partial_i \delta\sigma_I)^2 + \frac{1}{2} (m_\sigma^2 + 7\dot{\theta}_0^2) \delta\sigma_I^2 \right]. \quad (3)$$

The leading interaction Hamiltonian density is

$$\mathcal{H}_2^I = -c_2 a^3 \delta\sigma_I \dot{\delta\theta}_I, \quad (4)$$

$$\mathcal{H}_3^I = c_3 a^3 \delta\sigma_I^3, \quad (5)$$

where  $c_2 = 2R\dot{\theta}_0$ ,  $c_3 = V'''/6$  are constants.

We quantize the fields  $\delta\theta_I$  and  $\delta\sigma_I$  in the momentum space  $\mathbf{p}$ ,  $\delta\theta_{\mathbf{p}}^I = u_{\mathbf{p}} a_{\mathbf{p}} + u_{-\mathbf{p}}^* a_{-\mathbf{p}}^\dagger$ ,  $\delta\sigma_{\mathbf{p}}^I = v_{\mathbf{p}} b_{\mathbf{p}} + v_{-\mathbf{p}}^* b_{-\mathbf{p}}^\dagger$ , where  $a_{\mathbf{p}}$  and  $b_{\mathbf{p}}$  are independent of each other and each satisfies the usual commutation relation. The mode functions in terms of the conformal time  $\tau = \int dt/a(t)$  are

$$u_{\mathbf{p}} = \frac{H}{R\sqrt{2p^3}} (1 + ip\tau) e^{-ip\tau}, \quad (6)$$

$$v_{\mathbf{p}} = -ie^{i(\nu+(1/2))(\pi/2)} \frac{\sqrt{\pi}}{2} H(-\tau)^{3/2} H_\nu^{(1)}(-p\tau), \quad (7)$$

where  $\nu = \sqrt{9/4 - m^2/H^2}$  and  $m^2 = m_\sigma^2 + 7\dot{\theta}_0^2$ . As mentioned in the Introduction, the amplitude for the isocurvature mode  $v_{\mathbf{p}}$  decays as  $(-\tau)^{3/2-\nu}$  at late time  $\tau \rightarrow 0$ . If  $m^2/H^2 > 9/4$ ,  $\nu$  is imaginary,  $v_{\mathbf{p}}$  has an additional fast oscillating factor,  $\sim e^{\nu \ln(-p\tau/2)}$ , even after the horizon exit. This suppresses its contribution. We will consider the case  $0 \leq \nu < 3/2$ , i.e.,  $9/4 \geq m^2/H^2 > 0$ , in this paper.

The term that is responsible for the transformation from the isocurvature to curvature mode is (4). This introduces the ‘‘transfer vertex’’ [Fig. 1(a)]. The contribution from isocurvature to curvature correlation functions can therefore be computed according to the Feynman diagrams in Figs. 1(b) and 1(c). The term (5) is the leading source for large non-Gaussianities, since all other cubic interactions in the expansion involve  $\delta\theta$  which is in the slow-roll direction.

## III. BISPECTRA

We compute the three-point correlation function  $\langle \delta\theta^3 \rangle$ . The bispectrum  $\langle \zeta^3 \rangle$  is related to it through the usual time-delay relation  $\zeta \approx -H\delta\theta/\dot{\theta}$ .

The in-in formalism [4] gives

$$\langle \delta\theta^3 \rangle \equiv \langle 0 | \left[ \bar{T} \exp\left( i \int_{t_0}^t d\bar{t} H_I(\bar{t}) \right) \right] \delta\theta_I^3(t) \times \left[ T \exp\left( -i \int_{t_0}^t dt H_I(t) \right) \right] | 0 \rangle, \quad (8)$$

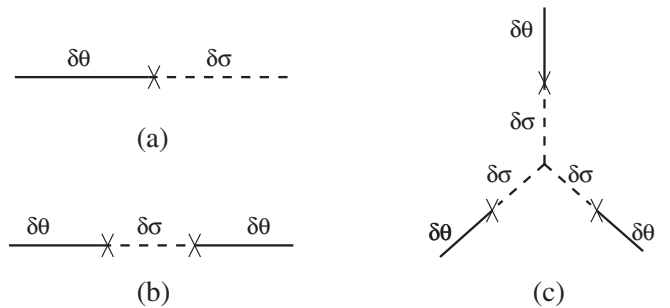


FIG. 1. Feynman diagrams for the transfer vertex (a), and the corrections from the isocurvature mode to the power spectrum (b) and bispectrum (c).

where  $t$  is the end of the inflation, and  $t_0$  is the infinite past. The  $H_I$  is the interaction Hamiltonian,

$$H_I = \int d^3\mathbf{x}(\mathcal{H}_2^I + \mathcal{H}_3^I). \quad (9)$$

One can directly expand the exponentials in (8). For our purpose, the relevant terms are those that involve four  $H_I$ 's. Each resulting quartic integral contains two ‘‘factors.’’ Each factor has an (anti-)time-ordered integration but there is no cross time ordering between the two. We call this form the ‘‘factorized form.’’ One can also rewrite all the integrands into one single time-ordered quartic integral,

$$\int_{t_0}^t dt_1 \int_{t_0}^{t_1} dt_2 \int_{t_0}^{t_2} dt_3 \int_{t_0}^{t_3} dt_4 \times \langle [H_I(t_4), [H_I(t_3), [H_I(t_2), [H_I(t_1), \delta\theta_I(t)^3]]]] \rangle. \quad (10)$$

We call this the ‘‘commutator form.’’ The Feynman diagram Fig. 1(c) corresponds to replacing one of four  $H_I$ 's in (8) or (10) with  $H_3^I$  and the rest of the three with  $H_2^I$ . A straightforward exercise of Wick contraction leads to, for the factorized form,

$$\begin{aligned} & -12c_2^3 c_3 u_{p_1}^* u_{p_2} u_{p_3}(0) \times \text{Re} \left[ \int_{-\infty}^0 d\tilde{\tau}_1 a^3 v_{p_1}^* u'_{p_1}(\tilde{\tau}_1) \right. \\ & \times \int_{-\infty}^{\tilde{\tau}_1} d\tilde{\tau}_2 a^4 v_{p_1} v_{p_2} v_{p_3}(\tilde{\tau}_2) \times \int_{-\infty}^0 d\tau_1 a^3 v_{p_2}^* u'_{p_2}(\tau_1) \\ & \times \left. \int_{-\infty}^{\tau_1} d\tau_2 a^3 v_{p_3}^* u'_{p_3}(\tau_2) \right] \times (2\pi)^3 \delta^3\left(\sum_i \mathbf{p}_i\right) \\ & + 9 \text{ other similar terms} + 5 \text{ permutations of } \mathbf{p}_i; \quad (11) \end{aligned}$$

and for the commutator form,

$$\begin{aligned} & 12c_2^3 c_3 u_{p_1}(0) u_{p_2}(0) u_{p_3}(0) \times \text{Re} \left[ \int_{-\infty}^0 d\tau_1 \int_{-\infty}^{\tau_1} d\tau_2 \right. \\ & \times \int_{-\infty}^{\tau_2} d\tau_3 \int_{-\infty}^{\tau_3} d\tau_4 \prod_{i=1}^4 (a^3(\tau_i)) \times a(\tau_2) (u'_{p_1}(\tau_1) - \text{c.c.}) \\ & \times (v_{p_1}(\tau_1) v_{p_1}^*(\tau_2) - \text{c.c.}) \times (v_{p_3}(\tau_2) v_{p_3}^*(\tau_4) u'_{p_3}(\tau_4) - \text{c.c.}) \\ & \times \left. v_{p_2}(\tau_2) v_{p_2}^*(\tau_3) u'_{p_2}(\tau_3) \right] \times (2\pi)^3 \delta^3\left(\sum_i \mathbf{p}_i\right) \\ & + 2 \text{ other similar terms} + 5 \text{ permutations of } \mathbf{p}_i. \quad (12) \end{aligned}$$

We write the argument  $\tau_i$  only once if they are all the same in one integrand, and the prime denotes the derivative respective to the conformal time  $\tau_i$ . The full details are presented in Ref. [11].

It is subtle to evaluate these integrals. Let us first look at the factorized form. In the UV limit,  $\tau_i \rightarrow -\infty$ , the integrands are fast oscillating. For the Bunch-Davies vacuum, the convergence of the integration is achieved by slightly tilting the contour clockwise or counterclockwise into the imaginary plane,  $\tau_i \rightarrow -\infty(1 \pm i\epsilon)$ . In fact, if the integration is convergent at IR,  $\tau_i \rightarrow 0$ , it is numerically much

more convenient to do a Wick rotation  $\tau_i \rightarrow iz_i$  for the left factor and opposite for the right. The integration range for  $z_i$  is from  $-\infty$  to 0. Now it is explicit that the integrand of each factor decays exponentially at UV. This is the case for  $0 \leq \nu < 1/2$ .

However, for  $1/2 < \nu < 3/2$ , using the asymptotic behavior of the mode functions, it is easy to see that each term in (11) is IR divergent. Physically, larger  $\nu$  corresponds to smaller  $m$  for the isocurvature mode. So the mode decays slower. The conversion from isocurvature to curvature mode lasts longer after the horizon exit. As we will see, this causes slower convergence in the IR, but not divergence.

Let us look at this in the commutator form (12). Because of the subtraction of the complex conjugate in various terms, the integrand decreases faster in IR. For example,  $u'_{p_1}(\tau_1)$  behaves as  $(-\tau_1)$  as  $\tau_1 \rightarrow 0$ ; but after subtracting off its complex conjugate, we have  $(-\tau_1)^2$ . The next two terms are slightly more complicated but similar. Since all these three terms are imaginary,  $v_{p_2} v_{p_2}^* u'_{p_2}$  in the 4th line must be imaginary to make the whole integration real. For  $\tau_{2,3} \rightarrow 0$ , the leading term of  $v_{p_2} v_{p_2}^* u'_{p_2}$  is real, so we need the subleading term in this limit. This also increases the IR convergence. Overall, it is not difficult to see that the IR convergence is achieved for all  $0 \leq \nu < 3/2$ . However, the Wick rotation no longer works in this form. The original integrands from the left and right factor have been multiplied together, so after Wick rotation, the exponential decay of some factors are cancelled by the exponential growth of the others.

To summarize, for  $1/2 < \nu < 3/2$ , the factorized form is well behaved in UV but encounters spurious divergence in IR in the intermediate step, while the commutator form is well behaved in IR but the UV convergence becomes tricky [12]. Therefore we have proved that the whole integral has no divergence. In fact, to see both types of convergence at once, we can choose a cutoff  $\tau_c$  in the middle, and make the whole expression take the factorized form in the UV,  $\tau_i < \tau_c$ , and commutator form in the IR,  $\tau_i > \tau_c$  [11]. This provides an efficient way to numerically calculate the shapes of the bispectra.

#### IV. SQUEEZED LIMIT AND SHAPE ANSATZ

We now look at the squeezed limit,  $p_3 \ll p_1 = p_2$ . In this limit, simple analytical expressions for shapes are possible. This can also help us construct simple analytical ansatz for the full shape, to facilitate future data analyses. In this limit, both Eqs. (11) and (12) become

$$\frac{c_2^3 c_3}{HR^6} \frac{1}{p_1^{(7/2)-\nu} p_2 p_3^{(3/2)+\nu}} s(\nu), \quad (13)$$

where  $s(\nu)$  is a  $p_i$ -independent numerical number, but involve complicated integrals [11]. The result is presented in Fig. 2.

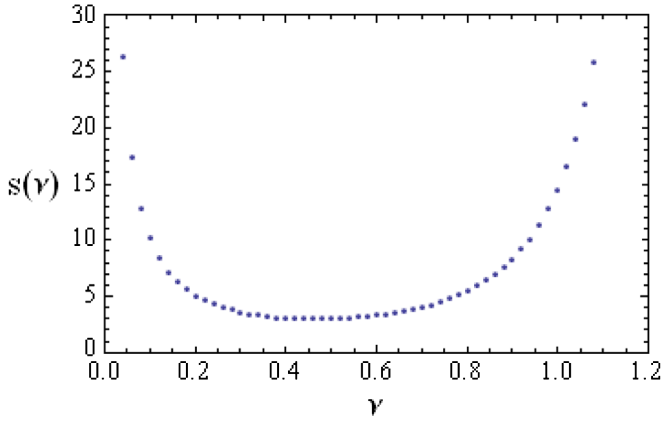


FIG. 2 (color online). The numerical coefficient  $s(\nu)$  in the squeezed limit.

Some comments are in order, to explain the behavior of  $s(\nu)$  near  $\nu = 0$  and  $\nu = 3/2$ . We have approximated the asymptotic behavior of  $H_\nu^{(1)}(-p_3\tau_i)$  in the small  $p_3$  limit as  $-i(2^\nu\Gamma(\nu)/\pi)(-p_3\tau_i)^{-\nu}$ . For very small  $\nu \sim 0$ , this requires  $p_3/p_1 \ll e^{-1/\nu}$ . So  $p_3$  needs to be increasingly small as  $\nu \rightarrow 0$ . Otherwise, if we fix a small  $p_3$ , near  $\nu = 0$  we should instead use  $i(2/\pi)\ln(-p_3\tau_i)$  as a better approximation. Therefore the rising behavior in Fig. 2 near  $\nu = 0$  does not mean that the non-Gaussianities are blowing up, rather signals the change of the shape to

$$\sim \frac{\ln(p_3/p_1)}{p_1^{7/2} p_2 p_3^{3/2}}. \quad (14)$$

As  $\nu \rightarrow 3/2$ ,  $m \rightarrow 0$ , the curvaton fluctuations do not decay, so its conversion to the curvature mode diverges in the constant turn case and an e-fold cutoff is necessary. Interestingly, in this limit, our shape approaches the local form, as expected from the multifield models studied in Refs. [5–9]. But here the non-Gaussianities can be made very large by having a large  $V'''$ , since we are not restricted to the slow-roll conditions even in the massless isocurvature limit.

Combining (13) and (14), a good ansatz for the full shape can be taken as, up to an overall amplitude,

$$-\frac{(p_1 p_2 p_3)^{-3/2}}{(p_1 + p_2 + p_3)^{3/2}} N_\nu \left( \frac{8 p_1 p_2 p_3}{(p_1 + p_2 + p_3)^3} \right), \quad (15)$$

where  $N_\nu$  is the Neumann Function. This ansatz gives an overall good match with the numerical results [11].

Note that in the squeezed limit, this one-parameter family of shapes goes as  $p_3^{-3/2-\nu}$ . This interpolates between the equilateral form,  $p_3^{-1}$ , and the local form,  $p_3^{-3}$  [13], so we call it the ‘‘intermediate form.’’ Two examples of the shape ansatz are shown in Fig. 3.

For comparison, we look at the three-point function of the isocurvature modes,  $\langle \delta\sigma^3 \rangle$ . Evaluating it after the horizon exit, we find that its amplitude is decaying and its shape goes as  $p_3^{-2\nu}$  in the squeezed limit. So at least in this model, the shape of the correlation function is changed

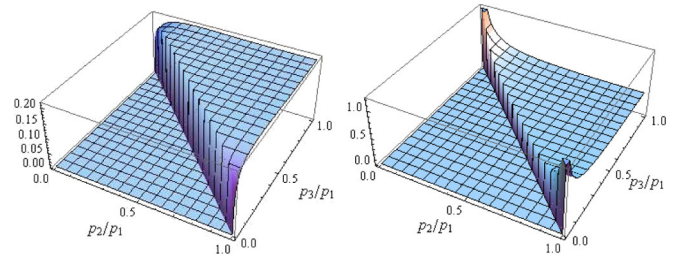


FIG. 3 (color online). Shapes of bispectra with intermediate form: (1) quasiequilateral ( $\nu = 0.2$ ), (2) quasilocal ( $\nu = 1$ ). The amplitudes are normalized by a factor of  $(p_1 p_2 p_3)^2$  to be dimensionless.

during the transfer. It is important to study this aspect in other multifield models, such as [14].

## V. SIZE OF NON-GAUSSIANITIES

The size  $f_{NL}$  of a bispectrum is defined by taking the equilateral limit [15],

$$\langle \zeta^3 \rangle \rightarrow \frac{9}{10} f_{NL} \frac{1}{p_1^6} P_\zeta^2 (2\pi)^7 \delta^3 \left( \sum \mathbf{p}_i \right), \quad (16)$$

where  $P_\zeta$  is the power spectrum. Using the relation  $\zeta = -H\delta\theta/\dot{\theta}$  and  $P_\zeta = H^4/(4\pi^2 R^2 \dot{\theta}_0^2) \approx 6.1 \times 10^{-9}$ , we get

$$f_{NL}^{\text{int}} = \alpha(\nu) \frac{1}{P_\zeta^{1/2}} \left( \frac{-V''''}{H} \right) \left( \frac{\dot{\theta}_0}{H} \right)^3. \quad (17)$$

We investigate the order of magnitude of each factor. The  $\alpha(\nu)$  should be evaluated numerically, similar to  $s(\nu)$ , but now in the equilateral limit. For example it is  $\mathcal{O}(1)$  and positive near  $\nu = 0$ . If we require that, in  $V(\sigma)$ , the quadratic term dominates over the cubic interaction for  $\sigma \lesssim H$ , so that we can trust the mode function, we need  $|V''''|/H < (m_\sigma/H)^2 \sim \mathcal{O}(1)$ . The perturbative method we used gives restriction on the size of  $\dot{\theta}_0/H$  because this parameter determines the strength of the transfer vertex. For example, the correction to the power spectrum can be simply calculated using Fig. 1(b),  $\delta P_\zeta \sim (\dot{\theta}_0/H)^2 P_\zeta$  and it is scale invariant, so for it to be perturbative we need  $(\dot{\theta}_0/H)^2 \ll 1$ . It is possible that the non-Gaussianity is larger if  $\dot{\theta}_0/H \sim 1$ , but to trust the perturbative results in this paper,  $\dot{\theta}_0/H < \mathcal{O}(1)$ . Overall, we see that  $|f_{NL}^{\text{int}}| \ll \mathcal{O}(10^4)$ , and its sign is the opposite of  $V''''$ . It will be very interesting to constrain it using the current and future data [16]. It is also interesting to study what the natural values for  $V''''$  and  $\dot{\theta}_0$  are from a more fundamental theory.

## ACKNOWLEDGMENTS

We thank B. Chen, A. Guth, Q-G. Huang, and M. Li for helpful discussions and A. Frey for his participation in the early stage of this work. X.C. was supported by the US DOE under cooperative research agreement DEFG02-05ER41360. Y.W. was supported by NSFC, NSERC, and IPP.

- [1] A. H. Guth, Phys. Rev. D **23**, 347 (1981); A. D. Linde, Phys. Lett. **108B**, 389 (1982); A. J. Albrecht and P. J. Steinhardt, Phys. Rev. Lett. **48**, 1220 (1982).
- [2] E. J. Copeland *et al.*, Phys. Rev. D **49**, 6410 (1994); X. Chen, J. Cosmol. Astropart. Phys. 12 (2008) 009.
- [3] J. M. Maldacena, J. High Energy Phys. 05 (2003) 013; V. Acquaviva, N. Bartolo, S. Matarrese, and A. Riotto, Nucl. Phys. **B667**, 119 (2003); T. Falk, R. Rangarajan, and M. Srednicki, Astrophys. J. **403**, L1 (1993).
- [4] For review, see S. Weinberg, Phys. Rev. D **72**, 043514 (2005).
- [5] D. S. Salopek and J. R. Bond, Phys. Rev. D **42**, 3936 (1990).
- [6] C. Gordon, D. Wands, B. A. Bassett, and R. Maartens, Phys. Rev. D **63**, 023506 (2000).
- [7] N. Bartolo, S. Matarrese, and A. Riotto, Phys. Rev. D **64**, 083514 (2001); **64**, 123504 (2001).
- [8] F. Bernardeau and J. P. Uzan, Phys. Rev. D **66**, 103506 (2002); **67**, 121301 (2003).
- [9] M. Sasaki and E. D. Stewart, Prog. Theor. Phys. **95**, 71 (1996); D. H. Lyth and Y. Rodriguez, Phys. Rev. Lett. **95**, 121302 (2005); G. I. Rigopoulos, E. P. S. Shellard, and B. J. W. van Tent, Phys. Rev. D **73**, 083521 (2006); D. Seery and J. E. Lidsey, J. Cosmol. Astropart. Phys. 09 (2005) 011; F. Vernizzi and D. Wands, J. Cosmol. Astropart. Phys. 05 (2006) 019.
- [10] This requires  $m_\sigma > \dot{\theta}_0$ . The  $\dot{\theta}_0$  will cause a displacement for the vacuum expectation value, we can redefine the  $\sigma$  and  $R$  so that  $\sigma = 0$  is the effective minimum.
- [11] X. Chen and Y. Wang, arXiv:0911.3380.
- [12] More detailed discussions on the computational advantages and disadvantages of both forms can be found in Ref. [11].
- [13] D. Babich, P. Creminelli, and M. Zaldarriaga, J. Cosmol. Astropart. Phys. 08 (2004) 009; X. Chen, M. x. Huang, S. Kachru, and G. Shiu, J. Cosmol. Astropart. Phys. 01 (2007) 002.
- [14] D. Langlois, S. Renaux-Petel, D. A. Steer, and T. Tanaka, Phys. Rev. D **78**, 063523 (2008); F. Arroja, S. Mizuno, and K. Koyama, J. Cosmol. Astropart. Phys. 08 (2008) 015.
- [15] E. Komatsu *et al.* (WMAP Collaboration), Astrophys. J. Suppl. Ser. **180**, 330 (2009).
- [16] E. Komatsu *et al.*, arXiv:0902.4759.